MAUSAM, **70**, 1 (January 2019), 111-120

551.501.8

Applying simulated satellite pictures based on a sub-kilometre scale numerical weather prediction model to gain insights into the formation mechanism of quasi-2 dimensional cloud features

K. K. HON and P. W. CHAN

Hong Kong Observatory, Hong Kong, China

(*Received 10 April 2018, Accepted 26 February 2019*)

email : pwchan@hko.gov.hk

सार – अनुकरित मेघ चित्रों को उत्पन्न करने के लिए मौसम अनुसंधान और पूर्वानुमान मॉडल (600 मी. के क्षैतिजीय ग्रिड पर) के सब-किलोमीटर विभेदन कार्यान्वयन का उपयोग किया गया। फिर हिमवारी-8 सैटेलाइट से प्राप्त वास्तविक प्रेक्षणों के साथ इसकी तुलना की गई। उत्तर पूर्वी मॉनसून में जहाँ उच्च विभेदन मॉडल रन्स मिलते जुलते मेघ पैटर्न पुन: निर्मित करते हैं कनवेक्टिव रोल, समुद्र समीर फ्रंट क्वाजी-2 आयामी मेघ फीचरों के बनने के चुनिंदा मामलों पर विचार किया गया। फिर मेघ की लाइन्स से संबद्ध मौसम वैज्ञानिक परिघटना का अध्ययन करने के लिए मॉडल फील्डों का विश्लेषण और विस्तार के साथ किया गया। इससे मेघ फीचर के बनने की प्रक्रिया के बारे में कुछ दिलचस्प जानकारी मिली है। यह न्यूमेरिकल मॉडल के आधार पर अनुकरित उपग्रह चित्रों को उत्पन्न करने की उपयोगिता को दिखाता है।

ABSTRACT. A sub-kilometer resolution implementation of the Weather Research and Forecast (WRF) model (at horizontal grid spacing of 600 m) is used to generate simulated cloud images, which are then compared with actual observations by the Himawari-8 satellite. Selected cases of formation of quasi-2 dimensional cloud features are considered, including convective roll, sea breeze front and lower boundary layer convergence in northeast monsoon, where the high-resolution model runs are found to reproduce the corresponding cloud patterns. Model fields are then analysed to study the meteorological phenomena associated with the cloud lines in more detail. They are found to provide some interesting information about the formation mechanism of the cloud features. This points to the usefulness of generating simulated satellite images based on the numerical model.

Key words – NWP, Aviation Model (AVM), Satellite cloud imageries.

1. Introduction

With decreasing costs and improving power of high-performance computer systems, the use of fine-resolution numerical weather prediction (NWP) models, sometimes down to the sub-kilometer scale, is becoming more common place in short-term regional or specialised weather forecasts. One example of such a NWP model is the Aviation Model (AVM) used by the Hong Kong Observatory (HKO) (Wong *et al.*, 2013; Chan and Hon, 2016). AVM has two domains: the outer one with a spatial resolution of 600 m over the geographically complex Pearl River Estuary (PRE) region and the inner one with a resolution of 200 m around the Hong Kong International Airport. Apart from supporting aviation applications, the AVM could also be useful for public weather forecast, e.g., in the nowcast of surface winds and temperatures at the city level.

The traditional way of visualizing the NWP output is the generation of temperature, humidity and wind forecast charts at the various pressure levels. It is becoming more popular to generate NWP-based satellite images, e.g., based on the channels of Himawari-8 satellite over the southern China region. The simulated satellite pictures are useful in a number of ways:

(a) More direct visualization of the NWP output because weather monitoring and forecasting is making reference to the satellite images;

(b) Verification of NWP output so that the model results are justified by comparing the actual and simulated satellite pictures;

(c) If the NWP results are considered reasonable by the comparison in (b), the physical mechanisms of the generation of clouds could be studied in detail using the NWP model outputs.

In this paper, a brief description is made about AVM and the generation of AVM-based satellite images. The

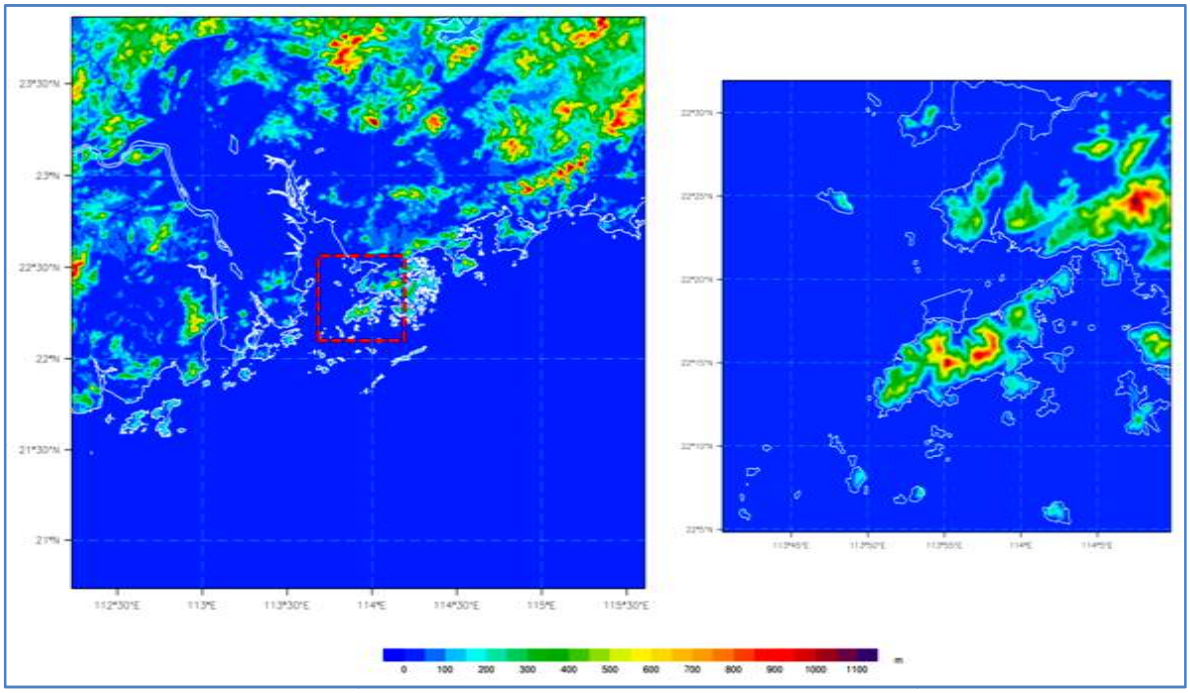

Fig. 1. Schematic diagram with terrain for model domains of AVM-PRD (left) and AVM-HKA (right)

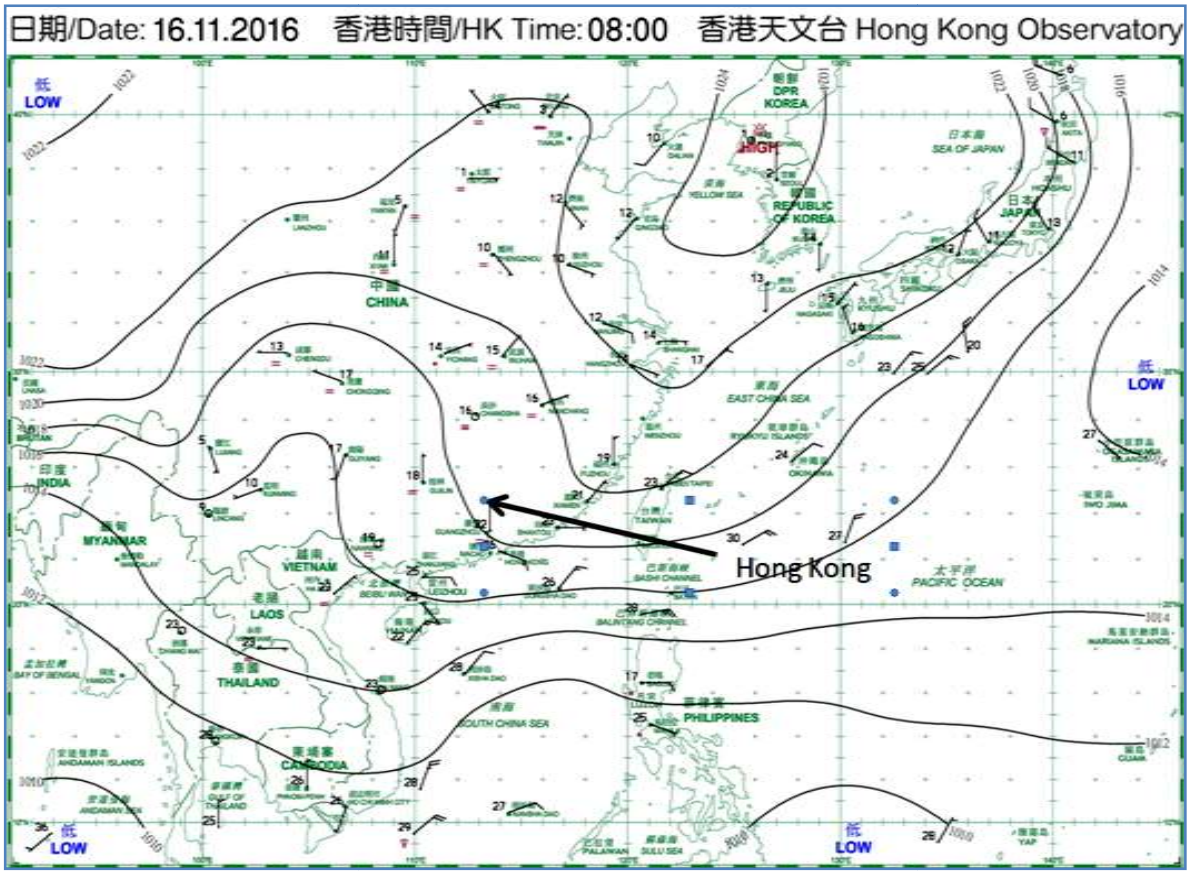

Fig. 2. Surface isobaric chart at 0000 UTC, 16 November, 2016

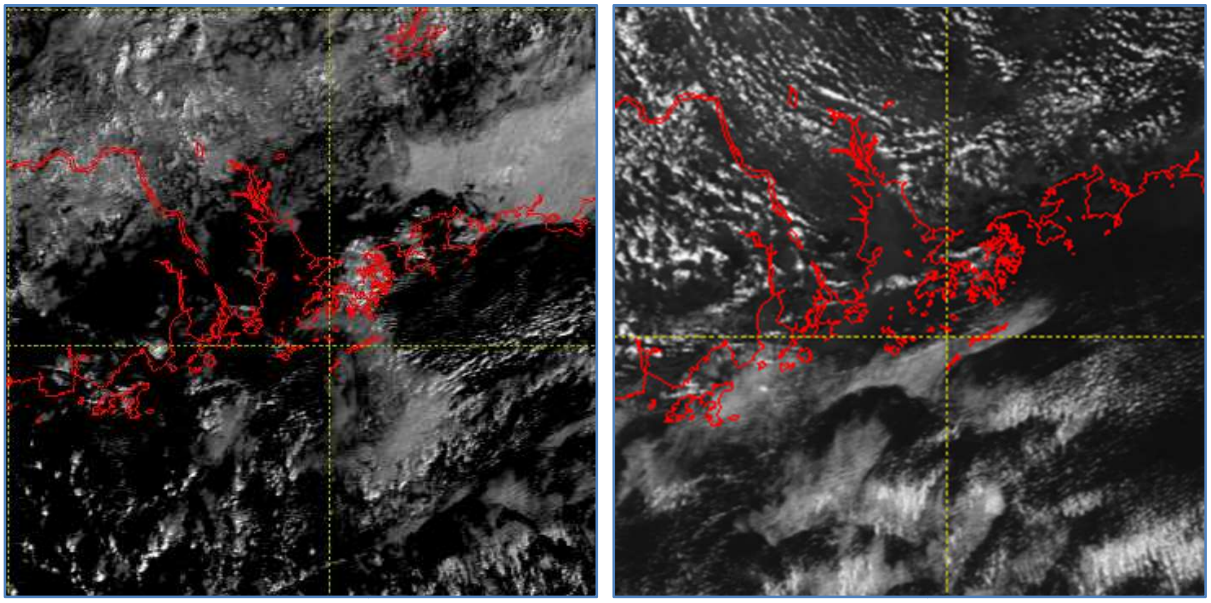

Fig. 3. Himawari-8 visible satellite images at 0000 UTC (Left panel) and 0600 UTC (Right panel), 16 November, 2016

major emphasis and the novel results are the understanding of quasi-two dimensional (quasi-2D) cloud features in the satellite images using AVM-output. Such quasi-2D features include convective rolls in fine weather, sea breeze front and wind convergence area within the boundary layer. The generation of cloud images for these features has not been discussed before over southern China, particularly with the use of sub-kilometre scale NWP model. Also the NWP outputs are considered to give new insights into the generation of these quasi-2D cloud features.

2. Model description

The Aviation Model (AVM) is a sub-kilometre resolution implementation of the Weather Research and Forecast (WRF) model (Skamarock and Klemp, 2007) for short-term, fine-scale forecasting in support of aviation operations at the Hong Kong International Airport (HKIA). The AVM comprises two singly-nested domains (Fig. 1):

(*i*) AVM-PRD covering the Pearl River Estuary region along the South China coastal areas at 600 m resolution; and

(*ii*) AVM-HKA covering the immediate vicinity of HKIA at horizontal resolution of 200 m. Both domains are hourly-updated and provide forecasts up to 9 hours ahead. Boundary conditions of the outer AVM-PRD, on which we focus in this paper, are taken from the latest available output of the RAPIDS-NHM, HKO's operational 2-km resolution mesoscale model (Wong and Chow, 2010), typically with a lag of 1-2 hours in initial time. Initial conditions to AVM-PRD are provided by 3D-Var analysis of conventional surface and upper air observations, as well as the dense surface observation network of the Guangdong province, based on first guess from the latest forecast of RAPIDS-NHM.

Given the high horizontal resolution, both cumulus convection and boundary layer turbulence are not parameterised in the existing AVM configuration *i.e.*, under so-called "explicit convection" and "LES" mode. Other key model settings include the Rapid Radiative Transfer Model for short- and long-wave radiation, the WRF double-moment microphysics scheme, the NOAH land surface model, as well as locally adapted terrain and land use data based respectively on the USGS 3-second topography and MODIS data sets.

3. Generation of simulated satellite cloud imageries

The simulated satellite cloud images featured in this paper are based on brightness temperature simulations using version 11.2 of RTTOV, a fast radiative transfer model (Saunders *et al.*, 1999). The computed brightness temperature values are based on spectral responses of the Advanced Himawari Imager (AHI), which is installed on board the recently launched Himawari-8 meteorological satellite of the Japan Meteorological Agency. The AHI is capable of operating at 16 different frequency bands with

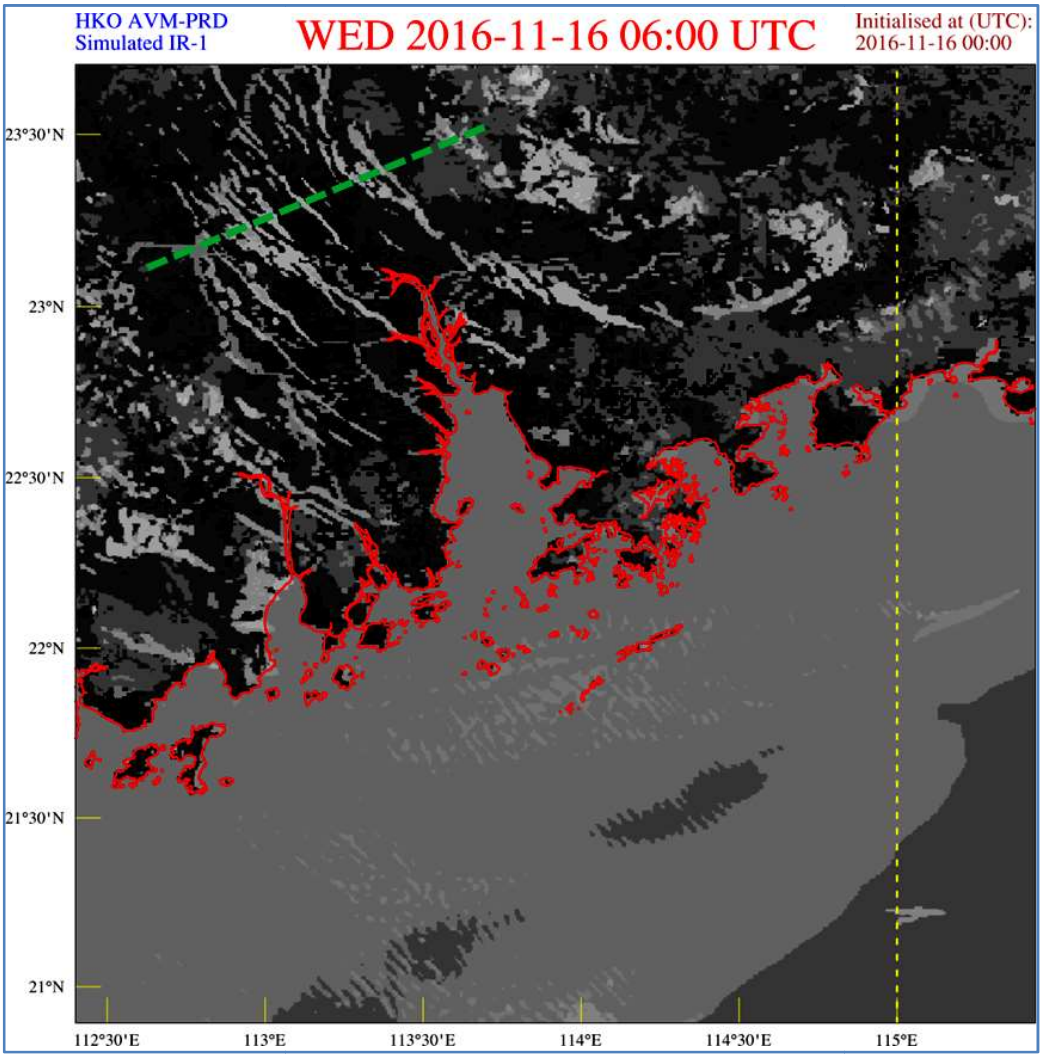

Fig. 4. Cloud distribution over the Pearl River Estuary as simulated using AVM-PRD model output. Here the AVM-PRD forecast is initialised at 0000 UTC, 16 November, 2016 and valid at 0600 UTC, which is the same as the observation time. The green line is the location of the vertical cross section in Fig. 6

central wavelengths ranging between 0.47 and 13.3 μm, from which the 10.4 μm channel (*i.e.*, corresponding to the IR1 infrared channel in the MTSAT-2IMAGER) would be considered in this paper.

RTTOV simulations are carried out using the three-dimensional fields of pressure, temperature, humidity, geopotential, liquid and solid hydrometeor mixing ratio from AVM-PRD output, as well as the two-dimensional fields of surface and skin temperatures. Cloud height and type required as input to the RTTOV code are then derived at each height of an atmospheric column using a combination of relative humidity and hydrometeor content. To speed up computations to suit real-time forecasting usage, each atmospheric column is treated independently without considering incident solar angle such that parallelization (e.g., using message parsing interface, MPI) could be achieved. The resulting cloudy radiance fields are then output at native model grid resolution (*i.e.*, 600 m for AVM-PRD).

4. Case studies

Three cases of quasi-2D cloud features are considered in this section. By verifying that the outer domain of AVM is giving reasonable results through comparison of the real and the simulated satellite images, the AVM outputs are used to study the features in detail from vertical cross sections across the 2D features.

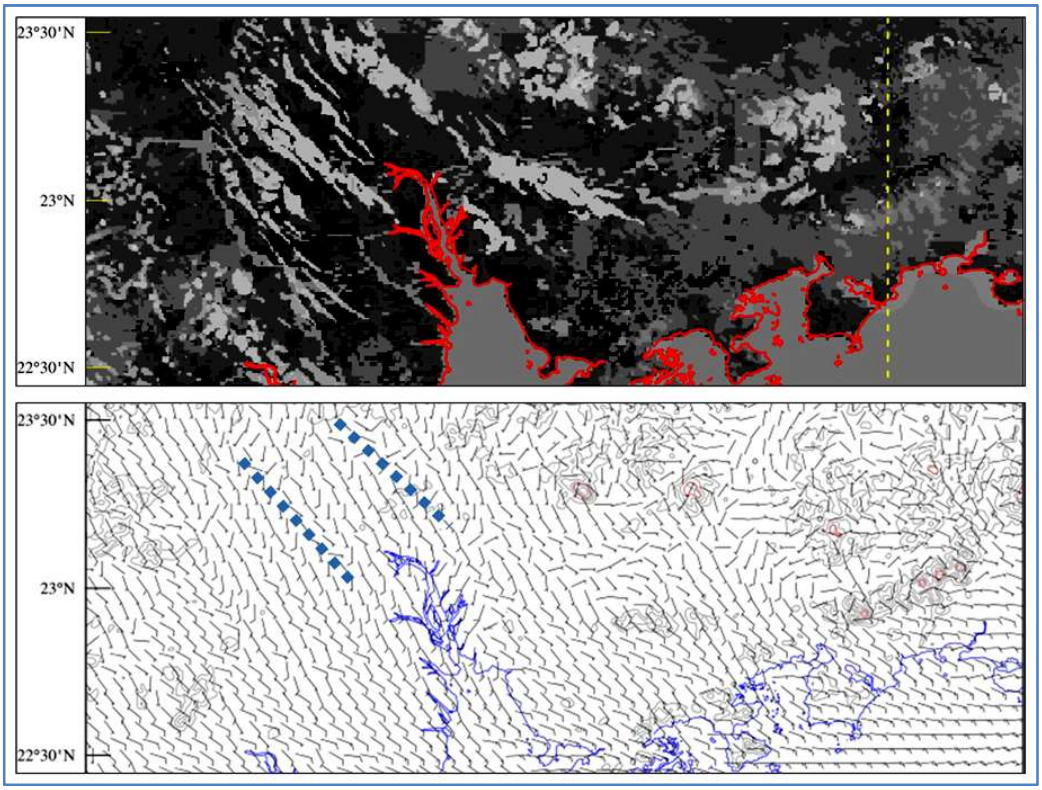

Fig. 5. Upper panel is an inset of Fig. 4, and the lower panel is the corresponding simulated surface wind field. The locations of surface wind convergence corresponding to the simulated cloud lines are shown as blue dotted lines

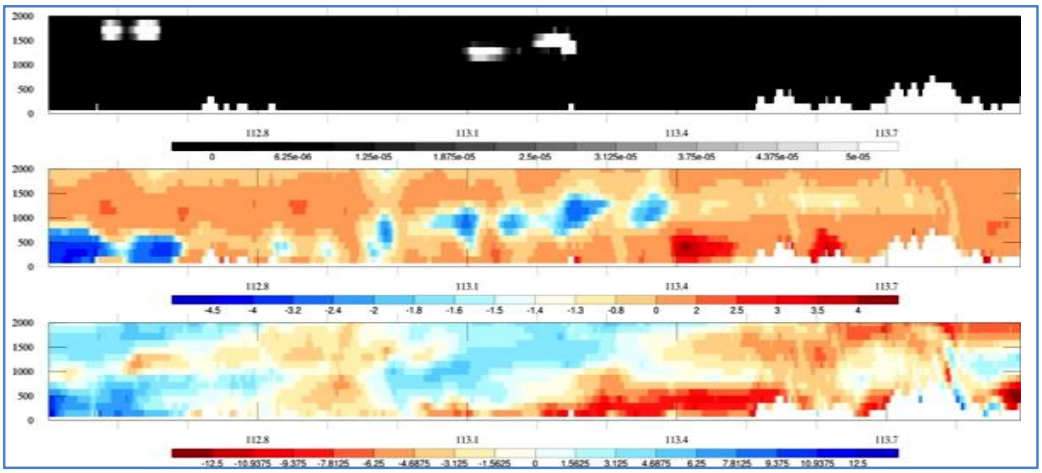

Fig. 6. Meteorological cross-section based on AVM-PRD output taken along the green dotted line in Fig. 4, from west to east: cloud liquid water mixing ratio (1st panel), zonal component of surface and upper-air winds (2nd panel, with asymmetric colour scale to highlight reversal in blue against background flow in red), and perturbation relative humidity (3rd panel, blue indicating positive deviation from the mean value at a particular altitude, red negative)

4.1. *Case 1: Convective roll*

The fine weather case of 16 November, 2016 is considered. From the surface weather chart at 0000 UTC (8 a.m. Hong Kong time, with HKT = UTC + 8 hours), Fig. 2, the PRE region has fine weather under the influence of a ridge of high pressure along the southeastern coast of China. The actual satellite pictures are shown in Fig. 3. In the morning (0000 UTC on that day), board bands of clouds are observed over inland areas

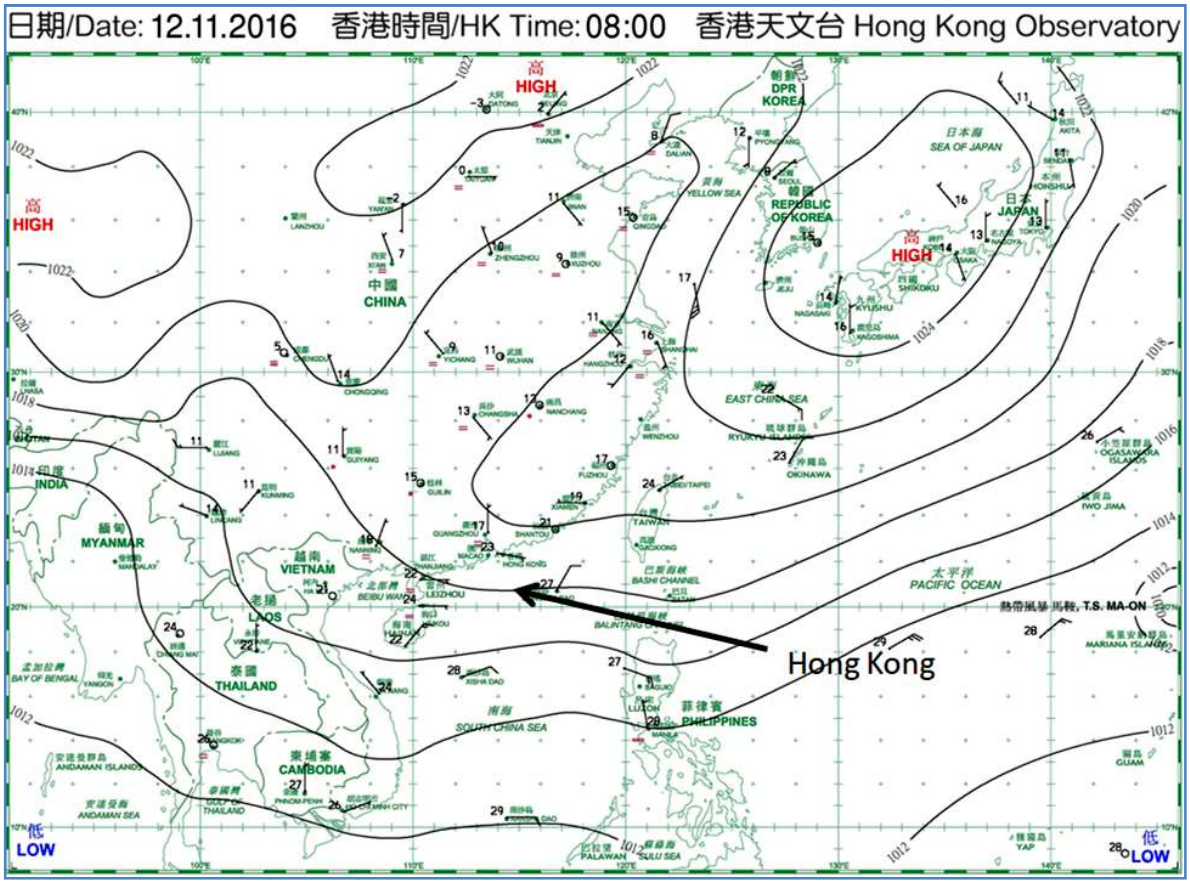

Fig. 7. Surface isobaric chart at 0000 UTC, 12 November, 2016

of southern China. In the early afternoon (0600 UTC on that day), a number of cloud lines are found in the same region. The cloud lines are following the direction of the wind in the lower troposphere. With the formation during the daytime, such cloud lines are believed to be arising from convective cloud rolls through surface heating.

The simulated satellite image at 0600 UTC on that day is shown in Fig. 4. Some of the cloud lines could be successful reproduced in the simulated image. The AVM is considered to perform reasonably well in representing the convection over land in this kind of weather condition.

The AVM outputs are studied in detail about the formation of the cloud lines. From Fig. 5, it could be seen that the cloud lines occur at areas with surface wind convergence. A cross section of the cloud line (location in Fig. 4) is shown in Fig. 6. The upper panel of Fig. 6 shows the location of the clouds. It can be seen that the clouds appear at locations with wind speed or direction convergence within the atmospheric boundary layer (ABL). It is interesting to note that there are a number of "blobs" of opposing wind direction (after taking the mean wind into account) and cloud formation is generally favoured at the location of the "blobs" as a result of the wind speed/direction convergence. The "blobs" may occur near the surface or in the middle of the ABL.

The cloud formation is also favoured at locations of higher humidity as noted in the relative humidity perturbation. In general, at higher relative humidity perturbation, the clouds would tend to form over there. However, quadrupole features of the wind direction in the ABL are not apparent in this case. It is interesting to note that the clouds do not form at locations with the quadrupole feature of surface convergence and upper level (but still within the ABL) divergence. As shown in the following examples, the quadrupole is more apparent in the sea breeze front. In any case, with the high spatial resolution of AVM, the simulated features of ABL are considered to give reasonable indication about the formation mechanism of the convective cloud rolls.

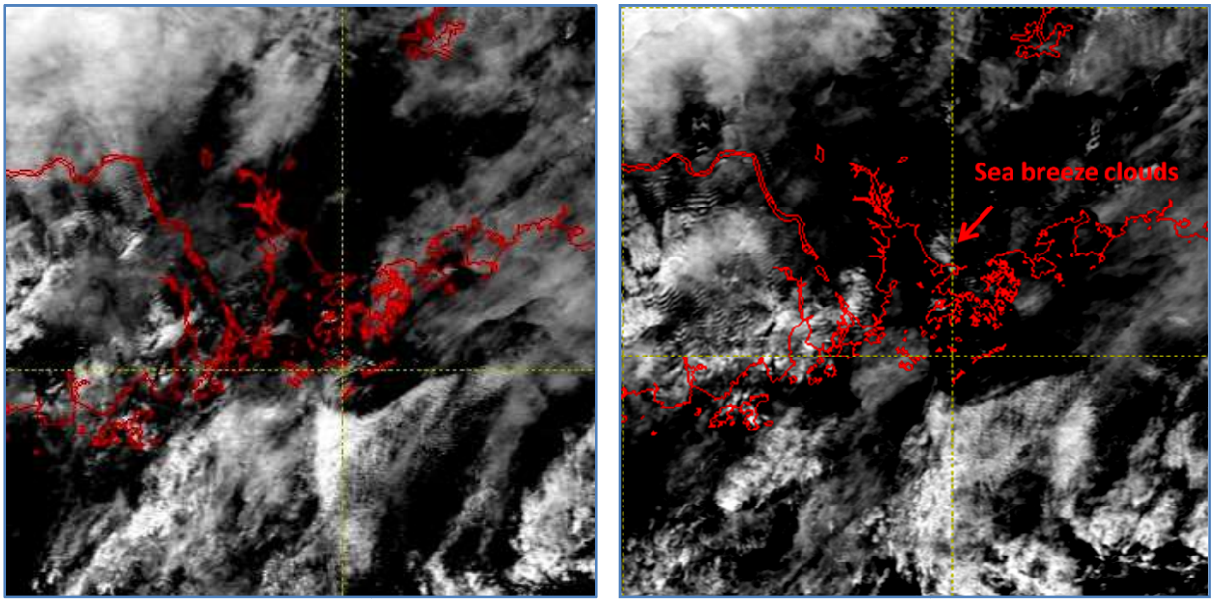

Fig. 8. Himawari-8 visibile satellite images at 0400 UTC (Left panel) and 0500 UTC (Right panel), 12 November, 2016

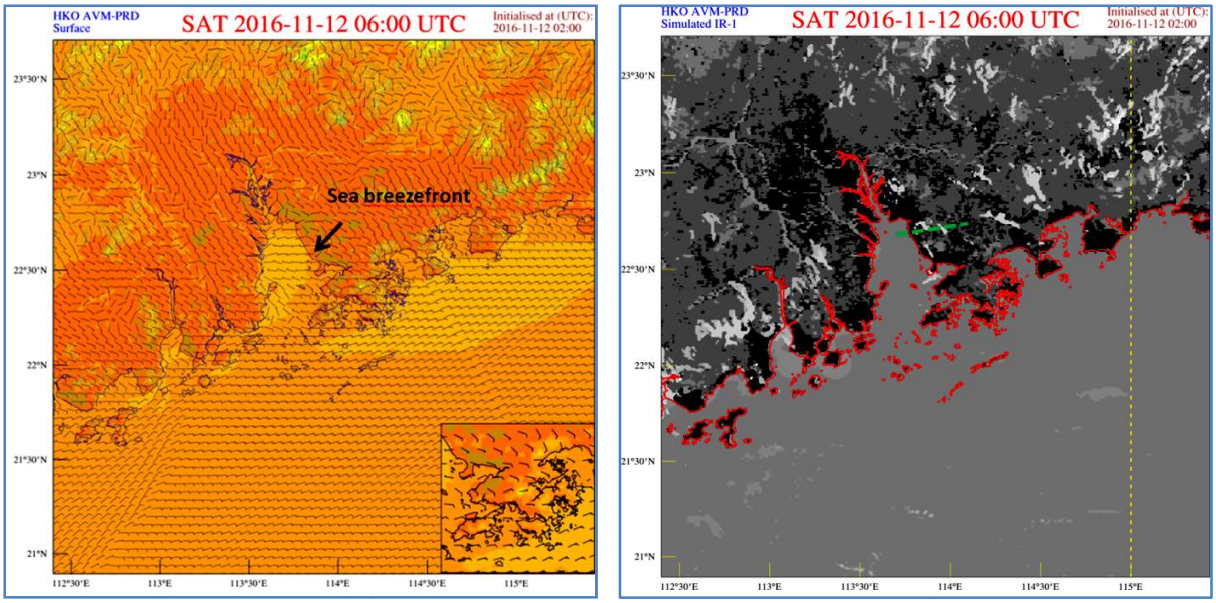

Fig. 9. The simulated surface temperature and wind field (Left panel) and simulated satellite image (Right panel) at 0600 UTC, 12 November, 2016, for 4 hour forecast as initialized at 0200 UTC, 12 November, 2016. The dotted green line in the lower panel is the location of the cross section in Fig. 10

4.2. *Case 2: Sea breeze front*

From the surface weather chart at 0000 UTC, 12 November, 2016 (Fig. 7), the southern China was under the influence by a board area of high pressure, which brought about fine weather to the coastal area. At noon (0400 UTC), the satellite picture shows that there are no clouds over the eastern coast of PRE, near Shenzhen, China (Fig. 8). One hour later, a line of clouds is observed at that location (Fig. 8). Such clouds are believed to arise from the convergence of the background easterly winds and the sea breeze westerly winds (surface wind data not shown). They also appear in the actual simulated picture (Fig. 9). The surface wind convergence is clear in the simulated surface winds (Fig. 9).

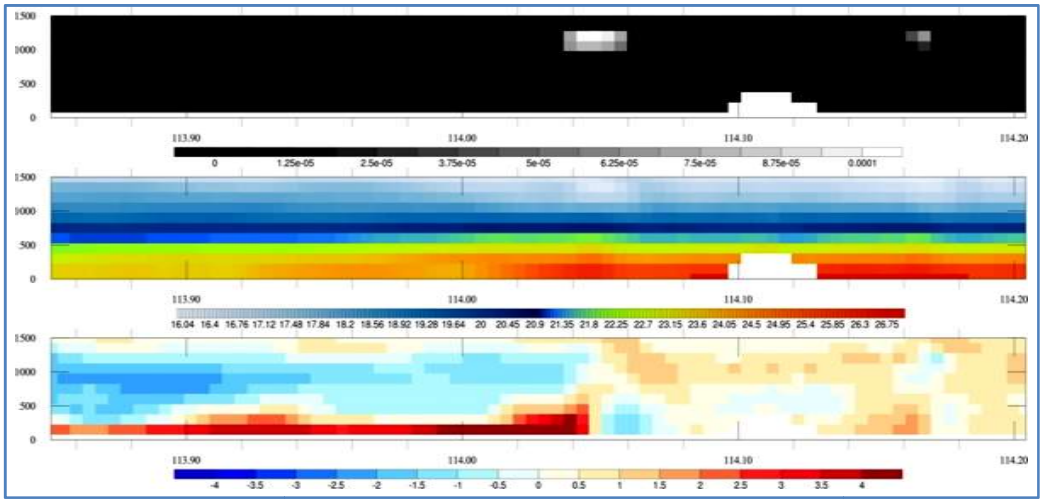

Fig. 10. Meteorological cross-section based on AVM-PRD output taken along the green dotted line, from west to east, in Fig. 9 for: cloud liquid water mixing ratio (1st panel), temperature (2nd panel) and zonal component of surface and upper-air winds (3rd panel, blue indicating easterly components, red westerly components)

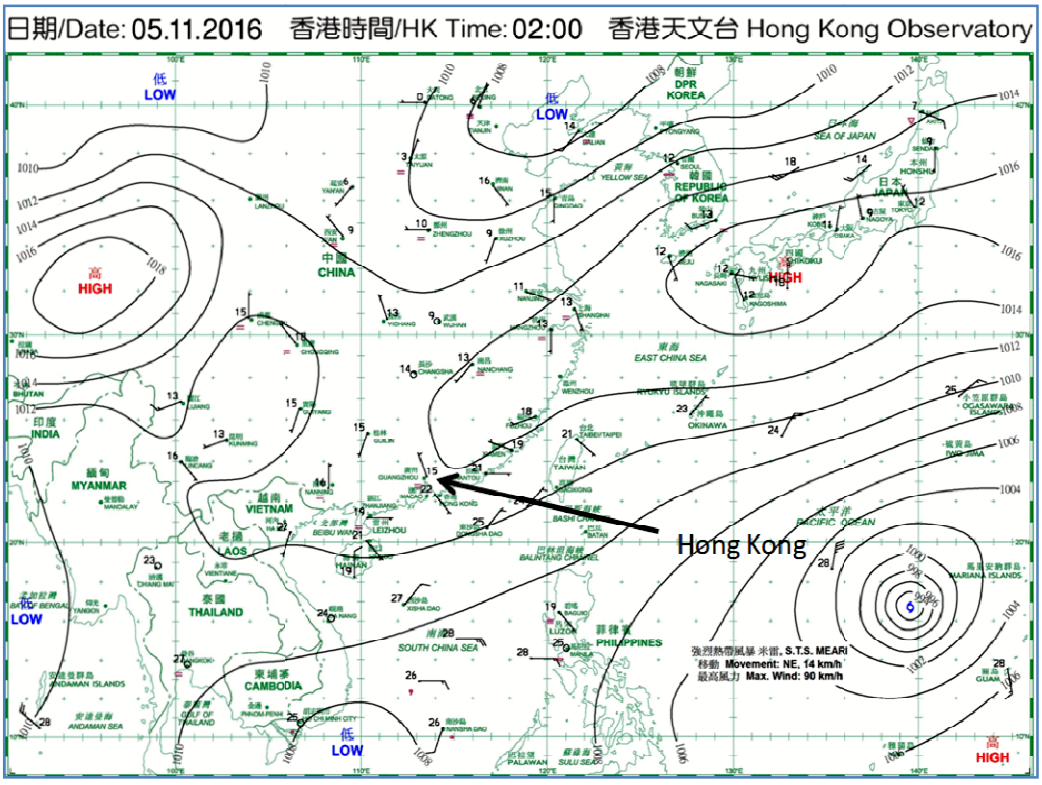

Fig. 11. Surface isobaric chart at 1800 UTC, 4 November, 2016

A vertical cross section (location in Fig. 9) of AVM outputs is given in Fig. 10. It can be seen that quadrupole feature of the winds within the ABL is rather clear in this case, at the location of the clouds. Also the temperature difference across the sea breeze front is readily observed, within higher temperature over the land than the sea. AVM appears to do a good job in capturing the main features of the sea breeze front.

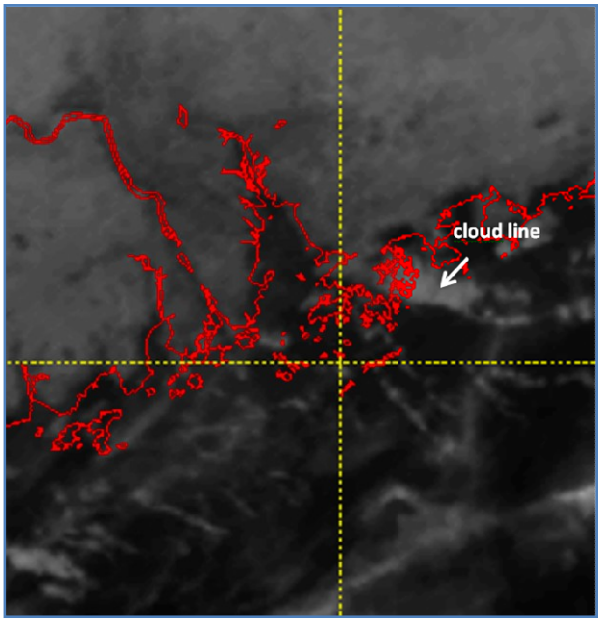

Fig. 12. Himawari-8 infrared image at 2100 UTC, 4 November, 2016

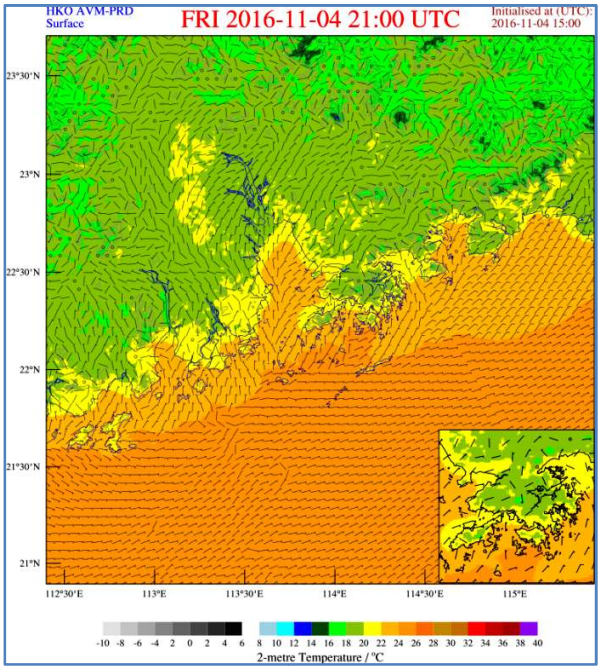

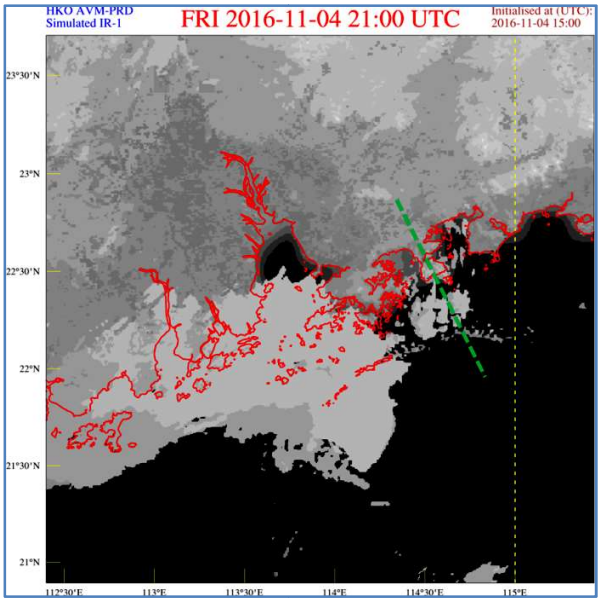

Fig. 13. The simulated surface temperature and wind field (upper panel) and the simulated satellite image (lower panel) validate 2100 UTC, 4 November, 2016, for AVM-PRD model initialized at 1500 UTC, 4 November, 2016. The dotted line in the lower panel indicated the location of the cross section presented in Fig. 14

The background easterly winds over land are warmer and converge with the cooler westerly sea breeze wind from the sea. The convergence between the background wind and sea breeze leads to the sea breeze front circulation in the form of a quadrupole. Water condensation occurs as the air rises in the convergence area, leading to the formation of clouds. The high spatial resolution of the AVM enables clear depiction of the formation mechanism of the sea breeze-related clouds.

4.3. *Case 3: Convergence between surface northeasterly and easterly winds*

From the surface weather chart in the early morning of 5 November, 2016 (Fig. 11), southern China was under the influence of the northeast monsoon. Easterly winds are prevailing over the south China coastal region. At the same time, northeasterly winds are spreading southward over PRE. They may converge with the background easterly to give rise to cloud feature. Such a line of clouds is observed from the actual satellite picture (Fig. 12). It is also apparent from the simulated cloud picture (Fig. 13). From AVM, the clouds do appear at a location with the convergence between the surface northeasterly and easterly winds (Fig. 13).

A vertical cross section across this quasi-2D cloud feature (location in Fig. 13) is given in Fig. 14. The clouds are observed to form at a location with surface wind convergence, temperature gradient and higher humidity. The former two features appear from the surface up to a height of about 500 m. The AVM output vividly depicts the main features of the cloud formation.

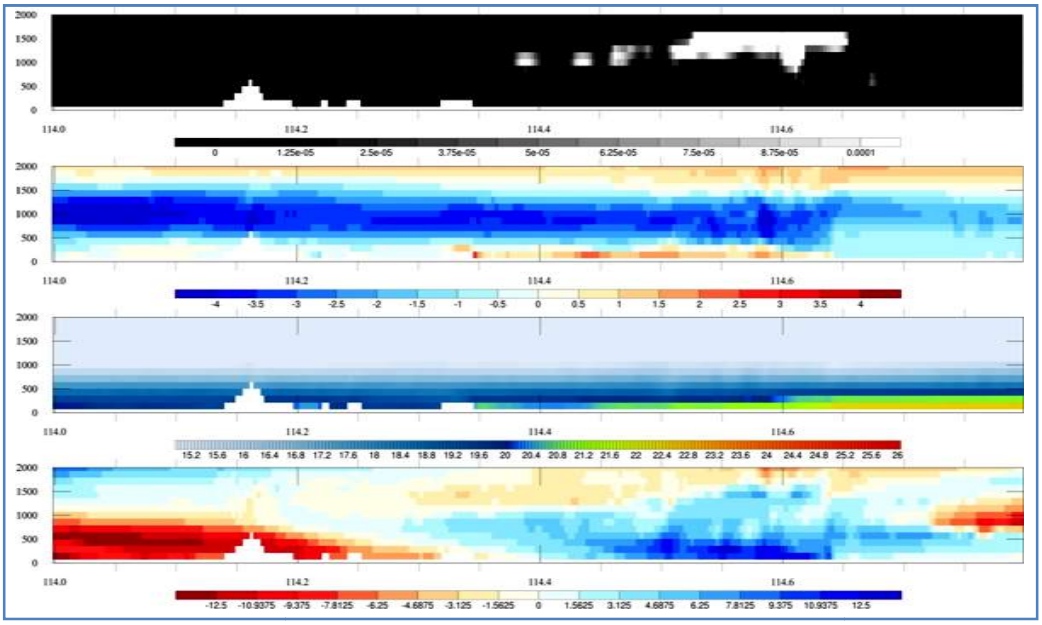

Fig. 14. Meteorological cross-section based on AVM-PRD output taken along the green dotted line, from west to east: cloud liquid water mixing ratio (1st panel), zonal component of surface and upper-air winds (2nd panel, blue indicating easterly components, red westerly components), temperature (3rd panel) and perturbation relative humidity (4th panel, blue indicating positive deviation from the mean value at a particular altitude, red negative)

The surface easterly winds of maritime origin is warmer, whereas the surface winds with more westerly component are of continental origin and slightly cooler. The warmer is forced to rise over the cooler air and condensation of the water vapour occurs, leading to cloud formation. Also, from the vertical cross section, it can be observed that the clouds are formed in an area of positive perturbation of relative humidity. Thus the high resolution of AVM enables very interesting depiction of the formation of the clouds at the surface convergence line.

5. Conclusions

Simulated satellite images are generated using a 600 m resolution model based on WRF. In selected cases of quasi-2D cloud lines, they appear to capture cloud features that are observed in the actual satellite images. As such, the modelling results are applied to study the meteorological phenomena in more details by making vertical cross sections along the cloud lines. Some interesting features of the meteorological fields are obtained. It is hoped that the high resolution numerical model could shed some new lights in the generation of the cloud line features.

The examples as presented in the present paper are preliminary results only. More systematic comparison between the actual and simulated cloud images would be conducted and reported in future papers.

Disclaimer

It is also acknowledge that the contents and views expressed in this research paper/article are the views of the authors and do not necessarily reflect the views of the organizations they belong to.

References

Chan, P. W. and Hon, K. K., 2016, "Performance of super high resolution numerical weather prediction model in forecasting terrain-disrupted airflow at the Hong Kong International Airport: case studies", *Met. Apps*, **23**, 101-114. doi:10.1002/met.1534.

Saunders, R. W., Matricardi, M. and Brunel, P., 1999, "An improved fast radiative transfer model for assimilation of satellite radiance observations", *Quart. J. Roy. Meteor. Soc.*, **125**, 1407-1426.

Skamarock, W. C. and Klemp, J. B., 2008, "A time-split nonhydrostatic atmospheric model for weather research and forecasting applications", *J. Comp. Phys.*, **227**, 3465-3485.

Wong, Wai Kin and Chow, Chi kin, 2010, "The New Generation Numerical Weather Prediction System at the Hong Kong Observatory. The 24th Guangdong-Hong Kong-Macau Seminar on Meteorological Technology, Shenzhen, China, 20-22 Jan 2010.

Wong, Wai Kin, Lau, Cheong Shing and Chan, Pak Wai, "Aviation Model: A Fine-Scale Numerical Weather Prediction System for Aviation Applications at the Hong Kong International Airport," *Advances in Meteorology*, **2013**, 532475, doi:10.1155/2013/532475.